Aerosol and Air Quality Research

ORIGINAL RESEARCH
https://doi.org/10.4209/aaqr.230057

Development of a Cost-effective Adsorption Dryer for High-quality Aerosol Sampling

Simonas Kecorius [1,2], Leizel Madueño[2,3*], Susanne Sues[1], Josef Cyrys[1], Mario Lovrić[4], Mira Pöhlker[3], Kristina Plauškaitė[2], Lina Davulienė[2], Agnė Minderytė[2], Steigvilė Byčenkienė[2]

[1] Institute of Epidemiology, Helmholtz Zentrum München, 85764 Neuherberg, Germany
[2] Center for Physical Sciences and Technology (FTMC), LT-10257 Vilnius, Lithuania
[3] Leibniz-Institute for Tropospheric Research, 04318 Leipzig, Germany
[4] Centre for Applied Bioanthropology, Institute for Anthropological Research, 10000 Zagreb, Croatia

ABSTRACT

Due to their affinity to water, physical-chemical properties of aerosol particles depend highly on the ambient relative humidity (RH). Aerosol drying below 40% RH is recommended to minimize measurement artifacts, increase data quality, and make results from different environments comparable. Diffusion dryers (DD) are one of the most frequently used tools to lower RH in sampled air. This work presents a custom-built DD, its design, construction, and application. By using readily available materials and 3D printing, we were able to manufacture a high-quality, cost-effective DD that can be used in various measurement scenarios (e.g., long-term measurements, intensive field campaigns, laboratory studies, and applications with low-cost sensors). The DD is equipped with ports for desiccant regeneration using clean and dry air, eliminating the need for desiccant removal from the dryer. The field tests of the proposed DD showed that it could reduce RH from ambient 65% to < 5 and 15% at flow rates of 2.5 and 8.0 L min^{-1}, respectively. The transmission efficiency (TE) of 10–20 nm and > 20 nm aerosol particles is between 60–80% and > 80%, respectively. The presented DD is easily scalable, thus, can be adapted for multiple applications at a low cost without compromising the data quality.

Keywords: Atmospheric aerosol particles, Data quality assurance, Aerosol drying, Aerosol measurement, Diffusion dryer

OPEN ACCESS

Received: March 14, 2023
Revised: September 15, 2023
Accepted: January 12, 2024

* **Corresponding Author:**
madueno@tropos.de

Publisher:
Taiwan Association for Aerosol Research
ISSN: 1680-8584 print
ISSN: 2071-1409 online

1 INTRODUCTION

In the last decade, physical, chemical, and biological properties of the aerosol particles have been extensively investigated by researchers, elucidating complex aerosol effects on regional and global climate (Drugé *et al.*, 2021; Li *et al.*, 2022), human health (Gioda *et al.*, 2022), disease transmission (Piscitelli *et al.*, 2022; Pöhlker *et al.*, 2021), indoor/outdoor air quality (Stamp *et al.*, 2022), societal challenges (Chakraborty and Basu, 2021), as well as their applicability in geoengineering (Pope *et al.*, 2012), medicine (Edwards *et al.*, 2004), and nanotechnology (Biskos *et al.*, 2008). The choice of different quantitative or qualitative methods to investigate aerosol particle properties greatly depend on specific scientific tasks and research domains, which often extend beyond the borders of a single country (Laj *et al.*, 2020). As in other disciplines, the scientific advancement in the field of atmospheric research highly depends on data credibility.

To ensure the highest possible measurement data quality and comparability not only from intensive field campaigns but also long-term monitoring observations (e.g., Global Atmosphere Watch (GAW); The National Oceanic and Atmospheric Administration Federated Aerosol Network (NFAN), Andrews *et al.* (2019) and Laj *et al.* (2020), respectively) a great effort has to be dedicated

towards establishing harmonized measurement protocols and standardized operating procedures. Such as recommendations for in-situ aerosol measurements developed by World Meteorological Organization/Global Atmosphere Watch (WMO/GAW, 2016). In most aerosol in-situ measurement scenarios, the determination of aerosol particle physical-chemical properties starts with aerosol sampling from ambient air. In a protocol by WMO/GAW (2016), the ideal sampling system for aerosol particles must a) exclude precipitation from the aerosol sample; b) minimize losses in sampling lines; and c) ensure sample relative humidity (RH) below 40%. And while dedicated, cyclone- or impactor-based inlets, coupled with laminar flow, conductive, straight, vertical, and short tubing satisfy the majority of requirements for aerosol sampling, ensuring air flow relative humidity below 40% is not as trivial. The ability of aerosol particles to uptake water vapour (Swietlicki *et al.*, 2008) determines not only its physical-chemical properties and their climate relevance, but may also introduce undesirable artefacts to measurement data. Düsing *et al.* (2019) showed that some microphysical and optical measurement techniques are sensitive to RH (e.g., the ability of absorption photometers filter material to uptake water vapour). Shukla and Aggarwal (2022) have demonstrated that for beta-attenuation measurement technique (a method commonly used by environmental monitoring stations to measure aerosol particle mass concentration) sample RH shall be even lower than that recommended by WMO/GAW – less than 35%. Under uncontrolled RH sampling conditions, observed particle physical-chemical properties will be a function of aerosol liquid water, which besides particle hygroscopicity, is also dependent on multiple factors, such as time of the day, season, and geographical location. This is not ideal when the research focuses on the physical-chemical properties of dry aerosol particles and not aerosol liquid water content. Such a scenario is especially relevant in warm and humid environments, where climate-controlled measurement stations/containers (usually controlled to 21–24°C) are kept below ambient dew point temperature, which may lead to condensation of water in the sampling lines.

Several ways exist to dry aerosol, including membrane and diffusion dryers (DD); and drying by dilution and heating (WMO/GAW, 2016). The choice of the drying system for a specific task mainly depends on technical and scientific requirements, as well as system costs. For example, drying by dilution may not be feasible where aerosol loading is already low, while drying by heating can introduce additional artefacts to aerosol physical-chemical properties (e.g., evaporation of volatile particle constituents; Vecchi *et al.*, 2009). Contrarily, the benefits of membrane and DD over drying by heating or dilution made them one of the most popular means of drying the aerosol sample (Tuch *et al.*, 2009; Kecorius *et al.*, 2017a). Commercially available membrane (e.g., Environmental Sampling System Model 3031200 by TSI Inc., USA; Monotube Dryer Model MD-700 by Perma Pure LLC, US) and DD (Diffusion Dryer 3062 by TSI Inc., USA; Diffusion Dryer DDU 570 by TOPAS, Germany; Diffusion dryer by Handix Scientific, USA) offer effective, simple, and nearly maintenance-free aerosol drying (in short term). The main advantage of the DD over the membrane dryer is that DD does not require sheath air to create the RH gradient for drying to occur. This greatly reduces the complexity (a need for constant flow of dry and aerosol-free air) of DD and make them as a primary choice for short-term aerosol measurements. Some of commercially available DD with technical specifications are listed in Table S1. The main disadvantage of the silica gel-based DD is that the active material has to be replaced and/or regenerated once saturated with water. With that said, the need for labour-intensive desiccant replacement/regeneration can be eliminated by utilizing automated aerosol DD. The design and performance of such custom-built dryer was presented by Tuch *et al.* (2009). The presented aerosol drying system although was proven to be robust for both intensive and long-term measurements in challenging environments (Tuch *et al.*, 2009; Kecorius *et al.*, 2017a, 2017b), the built complexity (includes stainless steel machining and welding) requires huge efforts to replicate such a system. Moreover, as the cost of a single commercially available membrane or DD ranges from 1000 to over 3000 €, the custom-built automated drying system, as described by Tuch *et al.* (2009), will easily exceed 10,000 €. In high-quality aerosol measurement and monitoring set-ups such expenses may not seem to be significant, however, the increasing interest and development of low-cost sensors may soon present a scenario, when commercially available and custom-built aerosol drying solutions will cost tens to thousands of times more than the aerosol measurement equipment itself. To this day, although many aerosol research studies have used custom-built DD (e.g., Valiulin *et al.*, 2021;

Ardon-Dryer *et al.*, 2022), just a few of them has focused explicitly on the characterization of the drying systems (e.g., determining drying efficiency, particle losses), and only one study investigated the feasibility of low-cost dryer for aerosol conditioning (Chacón-Mateos *et al.*, 2022). Although the presented dryer costs were reported to be approx. 50 €, the drying method was chosen to be sample heating, which is not ideal for ambient aerosol measurements (WMO/GAW, 2016 report).

This work presents the design, construction, and performance evaluation of a low-cost adsorption aerosol dryer. The main goal of this work is to present a fast, simple, and cost-effective way to build a high-quality adsorption dryer using widely available materials and without need for extensive machining and welding. The presented drying system can be easily reproduced and down-/up-scaled to a wide range of flows.

2 METHODS

This section presents a detailed description of the design, construction, and performance evaluation procedures of the proposed cost-effective diffusion dryer. In the subsection 2.1 Design and flow simulation, technical considerations, computer-aided design (CAD) options, and computational fluid dynamic (CFD) simulations of the airflow are presented. The subsection 2.2 Construction of the diffusion dryer introduces the choice of materials and the manufacturing procedure (fused deposition modeling, FDM) of the dryer. Lastly, subsection 2.3 Evaluation of drying performance and aerosol losses presents an exemplary case of the manufactured cost-effective diffusion dryer with a focus on drying performance and aerosol particle transmission efficiency (TE). The flow simulation was performed in ANSYS Fluent CFD (ANSYS, Inc., USA). The CAD design was done in Fusion 360 (Autodesk, Inc., USA).

2.1 Design and Flow Simulation

The design of the single diffusion dryer unit is based on the description of a membrane dryer given in the WMO/GAW (2016) report with some differences. Similar to the membrane dryer, the presented diffusion dryer consists of inner and outer shells (Fig. 1(a)). In this set-up, air sample with RH above the desired value enters and leaves the dryer through inner shell. The desiccant is placed in between two shells to create an RH gradient, based on which, water molecules migrate from the sample and are adsorbed onto silica gel creating a drying effect. The key difference between the presented and the membrane dryers is the material used for the inner shell and the fact that in the case of membrane dryer, there must be a steady flow of purge gas at low dewpoint temperature (< -20°C). In a diffusion dryer, no purge gas is required to achieve drying. The proposed dryer (Fig. 1(a)) was designed to enable simple silica gel regeneration (using dry air) and the ability to combine multiple drying units into one autonomous drying system, similar to that presented by Tuch *et al.* (2009). The outer shell of the dryer is a plastic tube that is 620 nm in length (Fig. 1(a), Nr. 4; polypropylene; with inner and outer diameters of 72 and 75 mm, respectively), and fitted with custom-built caps (Fig. 1(a), Nr. 6). A polypropylene tube was chosen because of its low cost, availability, and ease of mechanical processing (cutting to desired length does not require specific tools and can be done with a sharp cutter). The custom-built tube caps include ports and holes for inlet/outlet tubing, compressed air inlet/outlet (Fig. 1(a), Nr. 7), and silica gel loading (Fig. 1(a), Nr. 5). The inner shell that is in contact with the aerosol consists of three components, all of which were chosen to be electrically conductive to eliminate aerosol losses due to electrostatic charges (Hays and Hood, 1970; Cunningham and Hood, 1974; Liu *et al.*, 1985). The dryer inlet and outlet are made of 3/8 inch, 35 mm long stainless steel tubing (Fig. 1(a), Nr. 1* and 1), which are connected to a funnel (Fig. 1(a), Nr. 2* and 2), and are wrapped in stainless steel mesh creating a drying chamber (Fig. 1(a), Nr. 3; stainless steel woven mesh with a square hole diameter of 0.25 by 0.25 mm; 620 mm in length; 22 mm inner diameter). The custom-made inlet and outlet funnels were designed to ensure a smooth flow transition between the inlet/outlet and the inner drying chamber (Fig. 1(b)).

The ANSYS Fluent CFD (ANSYS, Inc., USA) software was used to investigate complex flow fields inside the aerosol dryer (Fig. 1(b)). A hex-dominant mesh geometry of approx. 0.4 million elements was used in this study to achieve accurate results. The airflow in the dryer is modeled at a

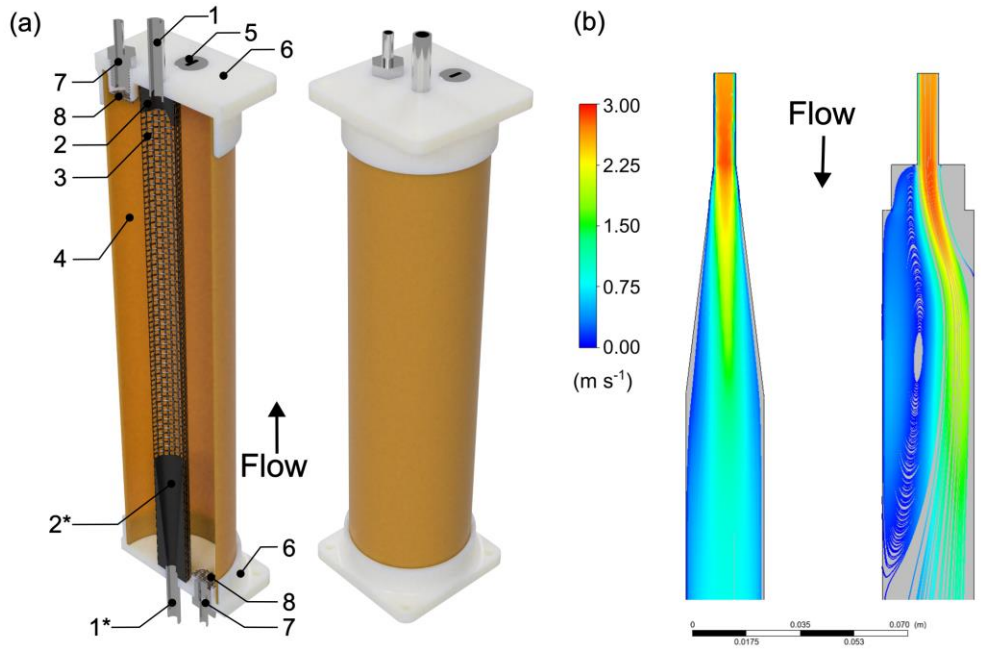

Fig. 1. 3D CAD model of the diffusion dryer (a) and air velocity contours (showing the velocity of the gas flow in m s^{-1}) from CFD simulation (b). Numbers 1–8 show dryer components: 1 – stainless steel inlet (1*) and outlet; 2 – conical inlet (2*) and outlet ports to constrain flow irregularities; 3 – drying chamber of stainless steel mesh; 4 – plastic tube; 5 – port for silica gel; 6 – plastic tube endings; 7 – compressed air inlet and outlet; 8 – stainless steel mesh.

constant flow of 8.0 L min^{-1}. The double precision simulations were steady state, with the solver 2023R1, turbulence model SST k-omega, 1000 iterations, and hybrid initialization. The SST k-omega turbulence model was used, because it shows a good prediction outcomes in terms of normalized vortex length, velocity streamlines, and velocity profile (Saha, 2021). The information from the CFD simulation was then used to optimize dryer geometry (length, inner and outer shell diameters, and dimensions of the inlet and outlet funnels) to achieve the best possible drier performance. An airflow simulation was performed for the inner dryer structure showing the aerosol chamber in 2D space (Fig. 1(b) left, proposed design; Fig. 1(b) right, conventional laboratory diffusion drier). The simulations for conventional diffusion drier showed both delaminarization of flow streamlines from the main flow and main flow path deviation from the center line towards the wall at a flow rate of 8.0 L min^{-1}. The flow irregularities occurred due to a sharp transition between airflow at the inlet and drying chamber (Fig. 1(b), right), which may result in increased aerosol particle losses. To mitigate the flow deflection effect, a smooth custom-designed funnel was fitted on both the dryer inlet and outlet. Based on the simulation results, funnel geometry was optimized for a flow rate of 8.0 L min^{-1} and a residence time of 1.5 s. The optimal length of inlet and outlet funnels was found to be 80 and 40 mm, respectively. The resulting flow of air in the dryer with custom-designed funnels showed no occurrence of flow irregularities (Fig. 1(b), left). To maintain laminar and smooth flow at higher flowrate, the corresponding funnels have to be longer, consequently increasing the length of the whole dryer. Increasing the residence time by the reduction of flow rate < 8.0 L min^{-1} does not require funnel modifications.

2.2 Construction of the Diffusion Dryer

To keep the cost of the DD low, while maintaining the highest possible quality, a few considerations have to be made when selecting the built materials and tools. Conventional machining (turning parts on lathe, milling and drilling, etc.), usually used for metal part manufacturing, requires professional knowledge and access to intricate tools. Both might not be available for the masses and are expensive. This limits the ability to produce conductive parts for the DD, which are required to reduce particle losses due to electrostatic charges (as described above). Fortunately, additive

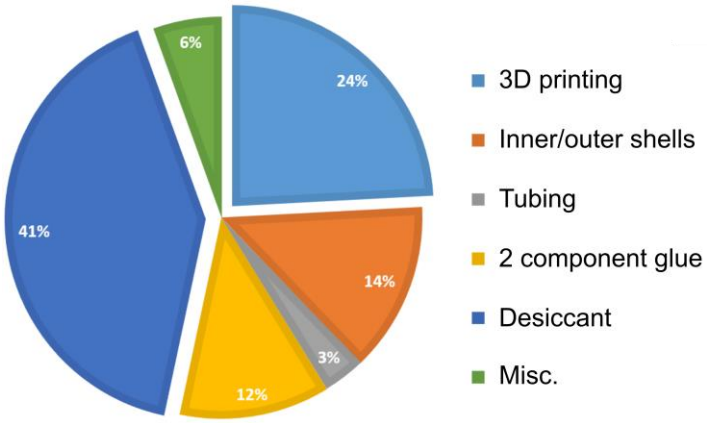

Fig. 2. The DD cost breakdown by component.

manufacturing (here referred to as 3D printing) can be used to create cost-effective, low-mechanical-load parts suitable for DD construction (Shahrubudin *et al.*, 2019). Which can considerably reduce manufacturing costs. However, it must be noted that DD parts in direct contact with aerosol must be made from a conductive material. This can be made possible using conductive filament (Kwok *et al.*, 2017; Marasso *et al.*, 2018). To manufacture tube endings (Fig. 1(a), part 6) and inlet/outlet funnels (Fig. 1(a), parts 2* and 2), we used fused deposition modeling 3D printer from FLSUN (model QQ-S Pro; Zhengzhou Chaokuo Electronic Technology Co., China). A technical (Prima Filaments, Netherlands) and electrically conductive (specific volume resistance of 24 Ω cm^{-1}; 3dk.berlin, Germany) polylactic acid (PLA) filaments were used to print non- (tube endings) and electrically conductive (funnels) parts, respectively. The 3D digital models were converted into a series of 2D instructions (toolpath) for 3D printer using open-source slicing software Cura (version 4.13, Ultimaker, Netherlands). Brass nozzle with 0.4 mm diameter hole, layer height of 0.1 mm, printing speed of 30 mm s^{-1}, and bed/nozzle temperature of 65/215°C were used to 3D print all the required parts. A step-by-step instruction to make DD (presented in this study) is provided in the supplementary materials (Fig. S1). Although not shown in this work, one can choose a transparent filament (e.g., Geeetech PETG Transparent, PolyLite PETG Transparent) making it possible to see when desiccant needs to be regenerated (if humidity sensor is not used; in a manual dryer regeneration mode).

Fig. 2 summarizes the cost breakdown of components used to manufacture the proposed cost-effective DD. Discernibly, silica gel (Lach-Ner d.o.o., Croatia) is the most expensive component of the DD, making approx. 40% of the total DD price. Second highest cost comes from the 3D printed parts. It must be mentioned that both silica gel and 3D printed parts costs may vary significantly. For example, we used a personal 3D printer in this work, reducing part costs to its minimum (only material costs). Custom 3D prints ordered from the public 3D printing services may increase 3D printing cost above 24%. On the other hand, cheaper silica gel and filament can be found, compensating for increased 3D printing costs. Overall, approximately 50 Euros was spent on materials used to assemble DD presented in this study, which is more than an order of magnitude cheaper than commercially available aerosol drying solutions.

2.3 Evaluation of Drying Performance and Aerosol Losses

The quality of an aerosol dryer depends on its drying performance and the losses of particles within the system. The performance of the DD developed in this study was tested under ambient conditions, over a span of a day, at the environmental monitoring station operated by Helmholtz Zentrum München (German Research Center for Environmental Health, Munich) and Environmental Science Center, Augsburg University, Augsburg, Germany (48.358°N, 10.907°E; Pitz *et al.*, 2008). During the tests, DD was attached to TROPOS-type Twin Mobility Particle Size Spectrometer (T-MPSS; Birmili *et al.*, 1999), measuring mobility particle number size distribution in a range from 5 to 800 nm. In this work, the design of DD was not optimized for particles below 10 nm. Because of this, TE was estimated in the size range from 10 to 800 nm. In total, 84 and 40 particle number

size distributions were recorded for 2.5 and 8 L min^{-1} flow rates, respectively. Half of those particle number size distributions were recorded with a dryer in a bypass. The experimental setup to evaluate DD performance is presented in Fig. S2. Aerosol inlet was equipped with a PM_{10} sampling head, designed to operate at 1 m^3 h^{-1}. An isokinetic flow splitter was used to split the airflow between the instruments. To estimate TE, the aerosol bypass (a stainless-steel tube with same length and flow velocity as DD) was installed in parallel to DD. Two automatic ball valves were used to switch between two lines (in 5-minute intervals), one of which was installed with DD. The relative humidity of sampled air was measured using an RH/T sensor (model HYT 939, Sensirion AG, Switzerland). The data was logged using a microprocessor (Arduino LLC, Italy) and Node-RED (IBM Emerging Technology, USA). To connect RH/T sensor to microprocessor and log the RH/T data, we used ChatGPT, a large language model developed by OpenAI, to generate code for both Arduino integrated development environment and Node-Red (https://chat.openai.com/, accessed: 2023-01-02). Prior performance evaluation, the dryer was tested for an absolute zero. The high efficiency particulate air filter was placed at the inlet of the T-MPSS system. Total particle number concentration, integrated from a particle number size distribution, was then observed. A total zero concentration was reached within < 2 min and did not increase for subsequent 5 scans (approx. 30 min).

3 RESULTS AND DISCUSSION

The average ambient relative humidity during the DD test period was 65.3 ± 1.4% (value after ± indicates one standard deviation). The drying ability of the DD was tested at two different flowrates—2.5 and 8.0 L min^{-1}, representing aerosol residence times of approx. 5 and 1.5 s inside the DD, respectively. At a flow rate of 2.5 L min^{-1}, the DD was able to remove 96% of the RH from ambient air (RH reduction from 64.5 ± 0.6% to 2.3 ± 0.2%; Fig. 3). At a higher flow rate of 8.0 L min^{-1}, the DD efficiency dropped to 79% (RH reduction from ambient 67.2 ± 0.5% to 14.3 ± 0.5% after DD). In a study by Tuch *et al.* (2009), authors have reported their developed diffusion dryer efficiency of 64.5% (aerosol RH reduction from ambient 78.5 to 27.1%). The reason for such a noticeably lower drying efficiency may be two fold. At first, during our dryer test, we have used a completely new and dry silica gel, which may have had higher water vapor adsorption, compared to dry air regenerated desiccant, used by Tuch *et al.* (2009). And secondly, we used a flow rate that is from 2 to more than 6 fold lower (versus 16.67 L min^{-1} or 1 m^3 h^{-1}). At a lower flow rate, less water vapor has to be adsorbed, resulting in a higher drying efficiency. When comparing our results to low-cost dryer based on heating (Chacón-Mateos *et al.*, 2022), it can also be seen that our proposed diffusion dryer has somewhat higher drying efficiency (79 to 96% versus 39 to 64%). It must be noted, however, that Chacón-Mateos *et al.* (2022) has defined dryer efficiency as a ratio between

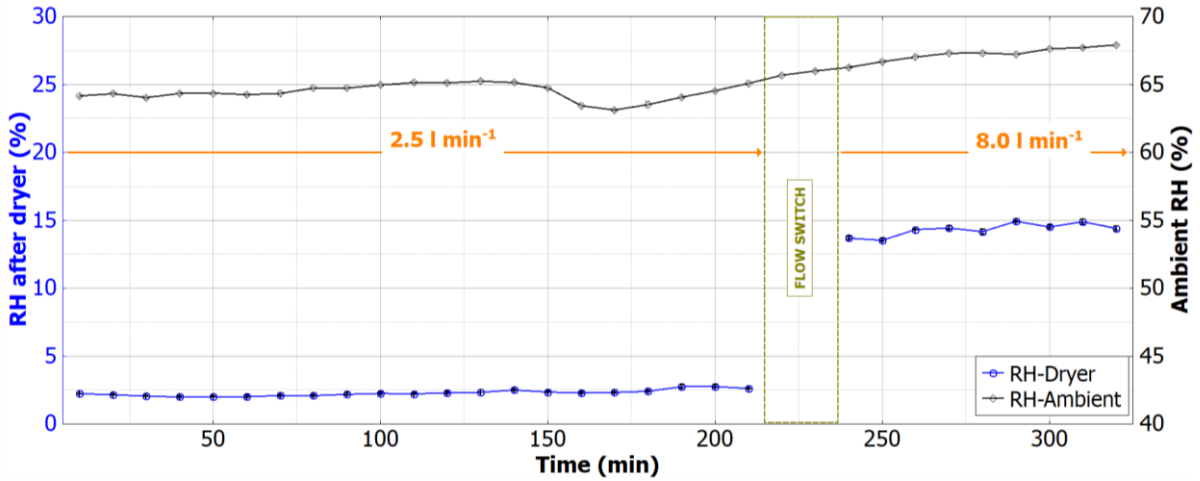

Fig. 3. DD performance evaluation using ambient aerosol at Augsburg environmental measurement station, Augsburg, Germany.

the aerosol particle mass concentration downstream versus upstream the dryer. Therefore, a direct comparison between drying efficiencies from two studies shall be taken with caution. It is worth noting that one of valuable aspects of the presented DD is an ability to be easily scaled depending on the sampling situation, measurement location, anticipated RH, and sampling period. For example, in central Europe, the summertime day temperature and RH of 28°C and 70%, respectively, are not uncommon (https://www.weatheronline.co.uk/). If the measurement container/device indoor/inside temperature is controlled to 21°C, the sampling line RH will reach 95.6% (https://www.lenntech.com/). In case the difference between ambient and instrument temperature is even greater (with instrument temperature < ambient temperature), the RH in sampling lines can exceed 100%, inducing condensation of water vapour and potentially damaging the measurement instrumentation (WMO/GAW, 2016). In such extreme cases, the aerosol shall be dried both in outdoor and indoor sampling lines and the desiccant would have to be replaced/regenerated rather frequently (requiring additional costs and labor). Because the DD is designed for easy desiccant regeneration using dry and clean compressed air, the DD can be extended to an autonomous aerosol drying system, a concept presented by Tuch *et al.* (2009). Two DDs, a set of ball valves (to control aerosol and drying air flow), RH and temperature sensors, as well as a microcontroller, can be arranged to automatically switch between two DD, with one being used to dry sample air, while the other is being regenerated. The cost of such a system can be reduced to a minimum using open-source software (e.g., Node-Red, IBM Emerging Technology, USA) to control the logics of the autonomous dryer; expensive automatic ball-valves can be replaced with a pair of manual ball-valve (e.g., Swagelok, USA) and high-torque servo motor (e.g., Feetech 35 kg servo, China), controlled with a microcomputer (e.g., Raspberry Pi, UK). The switching between two DDs shall be optimized depending on the particular situation. However, as a starting point, one could begin with RH independent switching between DD with a set time interval (e.g., 30 min). The code to control the valves with simple logic can be easily generated using ChatGPT, a large language model trained by OpenAI. With that said, an autonomous drying system using DD as a drying core will significantly increase the overall dryer price, thus, may not be suitable for low-cost applications.

The average TE of aerosol particles passing DD (in the size range from 10 to 800 nm mobility diameter) is presented in Fig. 3, and was between 60 and 80% for 10–30 nm and > 80% for > 30 nm particles, respectively. The average TE for total particle number concentration (integrated from measured particle number size distributions) over time was 80 ± 5% (one standard deviation) for 2.5L min^{-1} and 78 ± 4% (one standard deviation) for 8 L min^{-1}. The TE of ultrafine aerosol particles (diameter < 100 nm) at a flowrate of 2.5 L min^{-1} showed to be somewhat higher compared to 8.0 L min^{-1}. The same trend was also observed in the theoretical calculation of TE (including diffusion and sedimentation losses, inertial deposition in bends and contractions) using the methodology presented by von der Weiden *et al.* (2009). The difference between TE at different flow rates can be explained by increased diffusion losses at a lower flowrate (higher particle residence time in sampling lines). The asymptotic regression of the TE showed that the 50% penetration diameter is at approx. 5 nm. The larger particle (diameter above 1 micrometer) TE was not directly measured in this study (due to low super-micrometer particle concentration and lack of appropriate instrumentation). However, based on theoretical calculation following von der Weiden *et al.* (2009), the TE of super-micrometer particles is 99.9% (as long as the dryer is orientated vertically to reduce sedimentation losses). The performance (in terms of TE) of our proposed dryer is somewhat comparable to that by Tuch *et al.* (2009). In their study, the authors has reported a TE of 72 to 92% for > 3 nm and > 10 nm particles, respectively. The lower 50% penetration diameter was found to be < 3 nm. It can be seen that in general, a system developed by a Tuch *et al.* (2009) has a better TE towards smaller particles, which may be a result of higher aerosol flowrate. Unfortunately, the comparison of TE between low-cost dryers proposed in this study and that by Chacón-Mateos *et al.* (2022) is not possible, as the authors did not present size-dependent TE of their system.

The instances when the TE exceeded 100% (Fig. 4) were caused by irregularities in sampled ambient aerosol (e.g., ambient aerosol concentration during DD scan is slightly higher than the previous or consequent scan). An increasing scattering of the efficiency of large particles can be explained as follows. At lower particle number concentrations (at larger particle diameters) a small

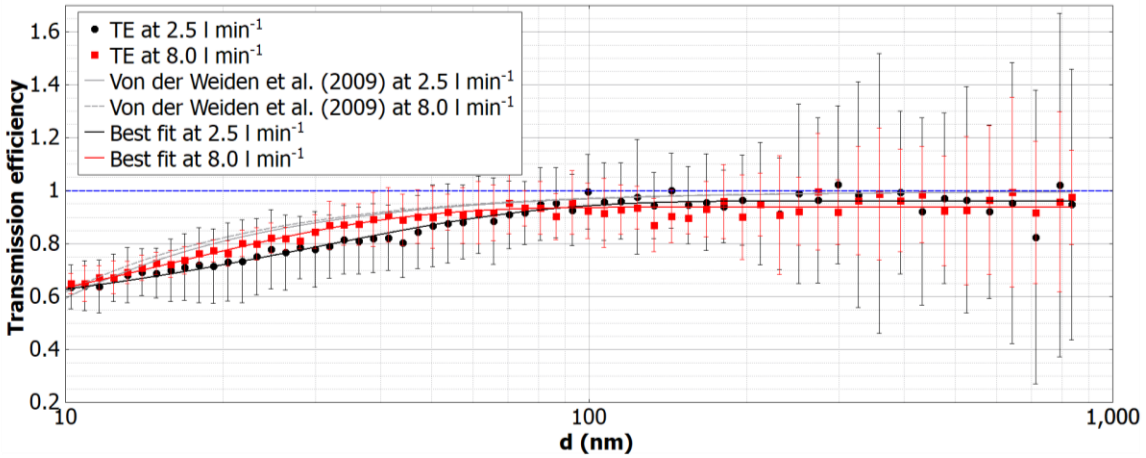

Fig. 4. Size-segregated transmission efficiency (TE). The TE was calculated as a ratio between aerosol passing diffusion dryer and aerosol bypass (see Fig. S2). Additionally, to experimental TE lines, a theoretical TE lines, calculated using formulas from von der Weiden *et al.* (2009), are presented by grey lines.

variation in particle number concentration results in relatively high standard deviation. In other words, at larger diameters, smaller particle number concentrations (Fig. S3) are highly sensitive to environmental perturbations influencing its concentration, thus, resulting in high standard deviation. In this work, TE standard deviation was calculated using the concept of propagation of uncertainty. In general, the designed DD showed a reasonable TE and ability to reduce ambient RH to the recommended value of < 40%.

4 CONCLUSIONS

The physical and chemical properties of the aerosol particles are highly dependent on the ambient relative humidity. To minimize RH-related artefacts and make aerosol properties measured in different environments comparable, it is important to control RH during aerosol sampling. Diffusion dryers (DD) are commonly used to lower the RH of sampled air in aerosol measurements below RH of 40%. Unfortunately, commercially available DDs can be costly and may be limited in their application range due to specific experimental requirements. Furthermore, none of the commercially available dryers are designed for use with low-cost sensors. This work presents a custom-built DD designed to be low-cost, high-quality, and easily adaptable for various measurement scenarios. The DD was constructed using readily available materials and 3D printing, making it an affordable alternative to commercial DDs. The dryer is equipped with ports for desiccant re-generation using clean and dry air, eliminating the need for desiccant removal from the dryer. The field tests of the custom-built DD showed that it effectively reduces RH from ambient levels of 65% to less than 5% and 15% at flow rates of 2.5 and 8.0 L min^{-1}, respectively. The TE of 10–30 nm and > 30 nm aerosol particles was found to be between 60–80% and > 80%, respectively. The low-cost design and scalability of the DD make it a viable option for long-term measurements, intensive field campaigns, laboratory studies, and for use with low-cost sensors without compromising data quality.

ACKNOWLEDGMENTS

This work has received funding from the Research Council of Lithuania (LMTLT), agreement No. S-MIP-22-57. The publication of this article was funded by the Open Access Fund of the Leibniz Association. The authors would like to acknowledge Augsburg University of Applied Sciences, Helmholtz Zentrum München (German Research Center for Environmental Health, Munich), and Environmental Science Center, Augsburg University for the access to the environmental measurement station in Augsburg, Germany.

SUPPLEMENTARY MATERIAL

Supplementary material for this article can be found in the online version at https://doi.org/10.4209/aaqr.230057

REFERENCES

Andrews, E., Sheridan, P.J., Ogren, J.A., Hageman, D., Jefferson, A., Wendell, J., Alástuey, A., Alados-Arboledas, L., Bergin, M., Ealo, M., Hallar, A.G., Hoffer, A., Kalapov, I., Keywood, M., Kim, J., Kim, S.W., Kolonjari, F., Labuschagne, C., Lin, N.H., Macdonald, A., *et al.* (2019). Overview of the NOAA/ESRL federated aerosol network. Bull. Am. Meteorol. Soc. 100, 123–135. https://doi.org/10.1175/BAMS-D-17-0175.1

Ardon-Dryer, K., Kelley, M.C., Xueting, X., Dryer, Y. (2022). The Aerosol Research Observation Station (AEROS). Atmos. Meas. Tech. 15, 2345–2360. https://doi.org/10.5194/amt-15-2345-2022

Birmili, W., Stratmann, F., Wiedensohler, A. (1999). Design of a DMA-based size spectrometer for a large particle size range and stable operation. J. Aerosol Sci. 30, 549–553. https://doi.org/10.1016/S0021-8502(98)00047-0

Biskos, G., Vons, V., Yurteri, C.U., Schmidt-Ott, A. (2008). Generation and sizing of particles for aerosol-based nanotechnology. KONA Powder Part. J. 26, 13–35. https://doi.org/10.14356/kona.2008006

Chacón-Mateos, M., Laquai, B., Vogt, U., Stubenrauch, C. (2022). Evaluation of a low-cost dryer for a low-cost optical particle counter. Atmos. Meas. Tech. 15, 7395–7410. https://doi.org/10.5194/amt-15-7395-2022

Chakraborty, J., Basu, P. (2021). Air quality and environmental injustice in India: Connecting particulate pollution to social disadvantages. Int. J. Environ. Res. Public Health 18, 1–14. https://doi.org/10.3390/ijerph18010304

Cunningham, R., Hood, H. (1974). Electrification due to the separation of materials. Digest of Literature on Dielectrics Volume 38 1974, IEEE, Washington, DC, USA, pp. 485–501. https://doi.org/10.1109/DLD.1974.7739037

Drugé, T., Nabat, P., Mallet, M., Somot, S. (2021). Future evolution of aerosols and implications for climate change in the Euro-Mediterranean region using the CNRM-ALADIN63 regional climate model. Atmos. Chem. Phys. 21, 7639–7669. https://doi.org/10.5194/acp-21-7639-2021

Düsing, S., Wehner, B., Müller, T., Stöcker, A., Wiedensohler, A. (2019). The effect of rapid relative humidity changes on fast filter-based aerosol-particle light-absorption measurements: Uncertainties and correction schemes. Atmos. Meas. Tech. 12, 5879–5895. https://doi.org/10.5194/amt-12-5879-2019

Edwards, D.A., Man, J.C., Brand, P., Katstra, J.P., Sommerer, K., Stone, H.A., Warded, E., Scheuch, G. (2004). Inhaling to mitigate exhaled bioaerosols. Proc. Natl. Acad. Sci. U.S.A. 101, 17383–17388. https://doi.org/10.1073/pnas.0408159101

Gioda, A., Beringui, K., Justo, E.P.S., Ventura, L.M.B., Massone, C.G., Costa, S.S.L., Oliveira, S.S., Araujo, R.G.O., Nascimento, N. de M., Severino, H.G.S., Duyck, C.B., de Souza, J.R., Saint Pierre, T.D. (2022). A review on atmospheric analysis focusing on public health, environmental legislation and chemical characterization. Crit. Rev. Anal. Chem. 52, 1772–1794. https://doi.org/10.1080/10408347.2021.1919985

Hays, D.A., Hood, H. (1970). Electrification due to the separation of materials. Digest of Literature on Dielectrics Volume 34 1970, IEEE, Washington, DC, USA, pp. 346–373. https://doi.org/10.1109/DLD.1970.7739915

Kecorius, S., Ma, N., Teich, M., van Pinxteren, D., Zhang, S., Größ, J., Spindler, G., Müller, K., Iinuma, Y., Hu, M., Herrmann, H., Wiedensohler, A. (2017a). Influence of biomass burning on mixing state of sub-micron aerosol particles in the North China Plain. Atmos. Environ. 164, 259–269. https://doi.org/10.1016/j.atmosenv.2017.05.023

Kecorius, S., Madueño, L., Vallar, E., Alas, H., Betito, G., Birmili, W., Cambaliza, M.O., Catipay, G., Gonzaga-Cayetano, M., Galvez, M.C., Lorenzo, G., Müller, T., Simpas, J.B., Tamayo, E.G.,

Wiedensohler, A. (2017b). Aerosol particle mixing state, refractory particle number size distributions and emission factors in a polluted urban environment: Case study of Metro Manila, Philippines. Atmos. Environ. 170, 169–183. https://doi.org/10.1016/j.atmosenv.2017.09.037

Kwok, S.W., Goh, K.H.H., Tan, Z.D., Tan, S.T.M., Tjiu, W.W., Soh, J.Y., Ng, Z.J.G., Chan, Y.Z., Hui, H.K., Goh, K.E.J. (2017). Electrically conductive filament for 3D-printed circuits and sensors. Appl. Mater. Today 9, 167–175. https://doi.org/10.1016/j.apmt.2017.07.001

Laj, P., Bigi, A., Rose, C., Andrews, E., Lund Myhre, C., Collaud Coen, M., Lin, Y., Wiedensohler, A., Schulz, M., A. Ogren, J., Fiebig, M., Gliß, J., Mortier, A., Pandolfi, M., Petäja, T., Kim, S.W., Aas, W., Putaud, J.P., Mayol-Bracero, O., Keywood, M., *et al.* (2020). A global analysis of climate-relevant aerosol properties retrieved from the network of Global Atmosphere Watch (GAW) near-surface observatories. Atmos. Meas. Tech. 13, 4353–4392. https://doi.org/10.5194/amt-13-4353-2020

Li, J., Carlson, B.E., Yung, Y.L., Lv, D., Hansen, J., Penner, J.E., Liao, H., Ramaswamy, V., Kahn, R.A., Zhang, P., Dubovik, O., Ding, A., Lacis, A.A., Zhang, L., Dong, Y. (2022). Scattering and absorbing aerosols in the climate system. Nat. Rev. Earth Environ. 3, 363–379. https://doi.org/10.1038/s43017-022-00296-7

Liu, B.Y.H., Pui, D.Y.H., Rubow, K.L., Szymanski, W.W. (1985). Electrostatic effects in aerosol sampling and filtration. Ann. Occup. Hyg. 29, 251–269. https://doi.org/10.1093/annhyg/29.2.251

Marasso, S.L., Cocuzza, M., Bertana, V., Perrucci, F., Tommasi, A., Ferrero, S., Scaltrito, L., Pirri, C.F. (2018). PLA conductive filament for 3D printed smart sensing applications. Rapid Prototyping J. 24, 739–743. https://doi.org/10.1108/RPJ-09-2016-0150

Piscitelli, P., Miani, A., Setti, L., De Gennaro, G., Rodo, X., Artinano, B., Vara, E., Rancan, L., Arias, J., Passarini, F., Barbieri, P., Pallavicini, A., Parente, A., D'Oro, E.C., De Maio, C., Saladino, F., Borelli, M., Colicino, E., Gonçalves, L.M.G., Di Tanna, G., *et al.* (2022). The role of outdoor and indoor air quality in the spread of SARS-CoV-2: Overview and recommendations by the research group on COVID-19 and particulate matter (RESCOP commission). Environ. Res. 211. https://doi.org/10.1016/j.envres.2022.113038

Pitz, M., Birmili, W., Schmid, O., Peters, A., Wichmann, H.E., Cyrys, J. (2008). Quality control and quality assurance for particle size distribution measurements at an urban monitoring station in Augsburg, Germany. J. Environ. Monit. 10, 1017–1024. https://doi.org/10.1039/b807264g

Pöhlker, M.L., Krüger, O.O., Förster, J.-D., Berkemeier, T., Elbert, W., Fröhlich-Nowoisky, J., Pöschl, U., Pöhlker, C., Bagheri, G., Bodenschatz, E., Huffman, J.A., Scheithauer, S., Mikhailov, E. (2021). Respiratory aerosols and droplets in the transmission of infectious diseases. arXiv:2103.01188 https://doi.org/10.48550/ARXIV.2103.01188

Pope, F.D., Braesicke, P., Grainger, R.G., Kalberer, M., Watson, I.M., Davidson, P.J., Cox, R.A. (2012). Stratospheric aerosol particles and solar-radiation management. Nat. Clim. Chang. 2, 713–719. https://doi.org/10.1038/nclimate1528

Saha, S. (2021). Numerical Simulation of Turbulent Flow Through a Sudden Expansion Channel: Comparison Between Three Models, in: Jha, K., Gulati, P., Tripathi, U.K. (Eds.), Recent Advances in Sustainable Technologies, Springer Singapore, Singapore, pp. 49–56. https://doi.org/10.1007/978-981-16-0976-3_6

Shahrubudin, N., Lee, T.C., Ramlan, R. (2019). An overview on 3D printing technology: Technological, materials, and applications. Procedia Manuf. 35, 1286–1296. https://doi.org/10.1016/j.promfg.2019.06.089

Shukla, K., Aggarwal, S.G. (2022). A technical overview on beta-attenuation method for the monitoring of particulate matter in ambient air. Aerosol Air Qual. Res. 22, 220195. https://doi.org/10.4209/aaqr.220195

Stamp, S., Burman, E., Chatzidiakou, L., Cooper, E., Wang, Y., Mumovic, D. (2022). A critical evaluation of the dynamic nature of indoor-outdoor air quality ratios. Atmos. Environ. 273, 118955. https://doi.org/10.1016/j.atmosenv.2022.118955

Swietlicki, E., Hansson, H.C., Hämeri, K., Svenningsson, B., Massling, A., Mcfiggans, G., Mcmurry, P.H., Petäjä, T., Tunved, P., Gysel, M., Topping, D., Weingartner, E., Baltensperger, U., Rissler, J., Wiedensohler, A., Kulmala, M. (2008). Hygroscopic properties of submicrometer atmospheric

aerosol particles measured with H-TDMA instruments in various environments - A review. Tellus Ser. B 60, 432–469. https://doi.org/10.1111/j.1600-0889.2008.00350.x

Tuch, T.M., Haudek, A., Müller, T., Nowak, A., Wex, H., Wiedensohler, A. (2009). Design and performance of an automatic regenerating adsorption aerosol dryer for continuous operation at monitoring sites. Atmos. Meas. Tech. 2, 417–422. https://doi.org/10.5194/amt-2-417-2009

Valiulin, S.V., Onischuk, A.A., Baklanov, A.M., Dubtsov, S.N., An'kov, S.V., Shkil, N.N., Nefedova, E.V., Plokhotnichenko, M.E., Tolstikova, T.G., Dolgov, A.M., Dultseva, G.G. (2021). Aerosol inhalation delivery of cefazolin in mice: Pharmacokinetic measurements and antibacterial effect. Int. J. Pharm. 607, 121013. https://doi.org/10.1016/j.ijpharm.2021.121013

Vecchi, R., Valli, G., Fermo, P., D'Alessandro, A., Piazzalunga, A., Bernardoni, V. (2009). Organic and inorganic sampling artefacts assessment. Atmos. Environ. 43, 1713–1720. https://doi.org/10.1016/j.atmosenv.2008.12.016

Von Der Weiden, S.L., Drewnick, F., Borrmann, S. (2009). Particle Loss Calculator - A new software tool for the assessment of the performance of aerosol inlet systems. Atmos. Meas. Tech. 2, 479–494. https://doi.org/10.5194/amt-2-479-2009

World Meteorological Organization/Global Atmosphere Watch (WMO/GAW) (2016). WMO/GAW Aerosol Measurement Procedures, Guidelines and Recommendations, GAW Report.